Int. J. Electrochem. Sci., 14 **(2019)** 2925 – 2932, doi: 10.20964/2019.03.78

International Journal of
ELECTROCHEMICAL
SCIENCE
www.electrochemsci.org

Electrochemical Characterization of poly(N-methylaniline) Films

Aziz Yağan

Chemistry Education, Dicle University, 21280, Diyarbakır, Turkey
E-mail: yagan@dicle.edu.tr

Received: 25 October 2018 / *Accepted:* 22 December 2018 / *Published:* 7 February 2019

Poly(*N*-methylaniline) (PNMA) films were obtained by cyclic voltammetry on Pt electrode in 0.1 M *N*-methylaniline dissolved in an electrolyte solution of 1.0 M HBF_4. Electrochemical characterization of the polymer films was investigated using electrochemical techniques like cyclic voltammetry and electrochemical impedance spectroscopy (EIS) in HBF_4 solutions. The influence of PNMA layer thickness and applied potential on impedance characteristics were also investigated. The results indicated that the electroactive behaviors of the films mainly depend on the polymer thickness and applied potentials.

Keywords: Poly(N-methylaniline); Electrochemical characterization; Impedance spectroscopy; Electrolyte effect

1. INTRODUCTION

The electrochemical impedance spectroscopy (EIS) technique has been widely used to study the electrochemistry of conducting polymer films. Especially, electrochemical doping/undoping process of conducting polymers have been investigated by using this technique. Electroactive polymers bearing different oxidation states continue to attract the interest of many scientists due to their various electrochemical properties, which make them amenable for use in a great variety of applications [1-7]. The impedance data can be analysed with a model. This model tries to describe the existence of capacitively and resistively coupled parallel electronic and ionic conduction paths within the polymer bulk and the metal/polymer interface [8].

PNMA exhibited different electrochemical behaviours when compared to polyaniline (PAni), which is mainly due to the block of the proton exchange sites by methyl substituents [9]. Therefore, the deprotonation of the imine groups in PAni during the second oxidation step couldn't be observed in PNMA. In other words, the absence of deprotonation in PNMA can prevent the formation of the pernigraniline (PA) state; hence, the absence of pernigraniline state in PNMA leads to a reduce in its degradation by hydrolysis during the electrochemical oxidation. Although PANI coated electrodes have been subjected to electrochemical characterization using cyclic voltammetry (CV) and EIS in aqueous acidic electrolytes [1]. However, to the best of my knowledge, detailed CV and especially EIS studies of PNMA films are unavailable in the literature. Therefore, the main purpose of this work is to achieve the electrochemical characterization of the PNMA by using CV and EIS techniques.

2. EXPERIMENTAL

N-methylaniline (BDH) was doubly distilled under vacuum and storage under inert atmosphere before use. HBF_4 (Merck) was used without further purification. CHI 660B electrochemical analyzer system was used for electrochemical polymerization and characterization of the corresponding polymer film coated on the electrode surface. Electrochemical studies were carried out in a conventional three-electrode cell at room temperature (ca. 25º C). Within a cell, a Pt disc, a Pt foil and a saturated calomel electrode (SCE) were used as a working, a counter and a reference electrode, respectively. PNMA films were grown onto Pt dics electrodes in 1.0 M HBF_4 solution containg 0.1 M NMA via CV between -0.20 V and 0.85 V vs SCE at a scan rate of 50 mV/s. 25, 50 and 75 repeating cycling were used in order to obtain various polymer film thickneses. During potentiodynamic electrolysis, the corresponding polymer films were obtained in their reduced states. After getting PNMA films, their electrochemical behaviors were investigated by using CV between -0.2 V and 0.85 V at various scan rates from 50 to 250 mV/s with an increment of 25 mV/s. In order to get reproducible results, the areas under cathodic peaks formed in the second scans were used to calculate voltammetric charge densities (Q_c) of the films in a monomer free electrolyte solution. EIS spectra were obtained for freshly prepared PNMA electrodes; the ac signal with an amplitude of 7 mV was applied in the 10^5 Hz to 10^{-1} Hz frequency range. PNMA films were equilibrated for at least 3-5 min at applied each E_{dc} before each EIS measurement. Before and after EIS measurements, the electrochemical properties and stability of the electroactive polymer film were checked by using cyclic voltammetry in the potential range from -0.20 V to 0.85 V.

3. RESULTS AND DISCUSSION

Potentiodynamic electropolymerization of NMA was performed successfully separately in electrolyte solutions of 1.0 M HBF_4 and 1.0 M H_2SO_4 in Figure 1. During anodic scan each cyclic voltammogram represented one irreversible oxidation peak, which is responsible from the electropolymerization of NMA on Pt electrode. The oxidation of NMA resulted in the formation of nucleation on the Pt substrate, and then electroactive polymer films were obtained on the electrode surface after successive potential cycles. The cyclic voltammetric growth of PNMA on Pt electrode showed one anodic peak at about 0.36 V after twelve cycles and the three cathodic peaks started to appear at about 0.26, 0.48 and 0.56 V. The reduction peak at about 0.56 V can be ascribed to the transformation of PNMA from emeraldine (EM) to leucoemeraldine (LE) form and the reverse transition takes place at about 0.26 V [1].

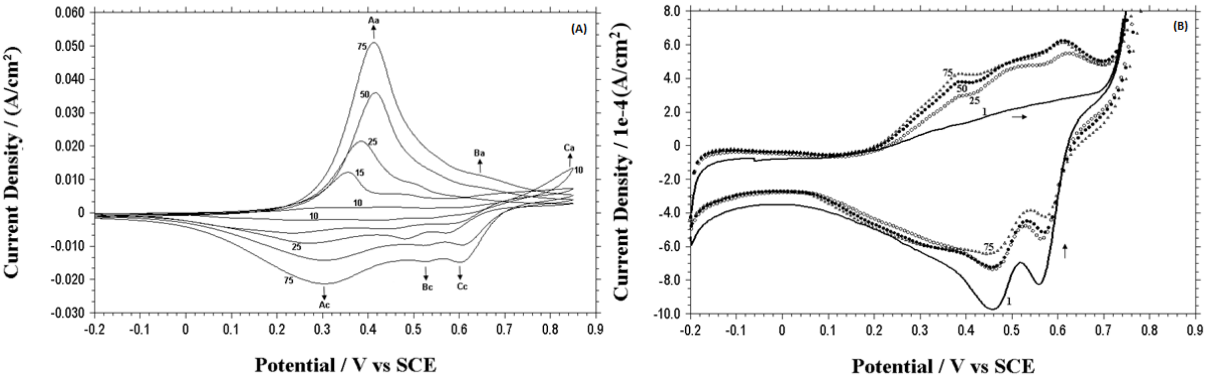

Figure 1. Potentiodynamic polarization curves of Pt electrode in (A) 1.0 M HBF_4 and (B) 1.0 M H_2SO_4 solution containing 0.1M NMA between -0.20 V and 0.85 V vs. SCE at a scan rate of 25 mV/s.

The type of electrolyte had significant influence on the growth and properties of polymer. Thus, the effect of H_2SO_4 as an electrolyte to electropolymerization was partially investigated. As can be seen in Figure 1 (B), the shape of curves with location and values of the anodic and cathodic current peaks was quite different according to obtained in HBF4 used as electrolyte. This behavior also was current in polymerization solution containing $HClO_4$ [4,6,10] and H_2SO_4 and HCl solution [10]. Figure 1 and Figure 2 showed that the growth of PNMA in an electrolyte solution of H_2SO_4 is very less compared to HBF_4 electrolyte solution. As additional information, the development of poly(N-buthylaniline) in HBF_4 is not similar to PNMA growth. The use of N-buthyl aniline instead of NMA as monomer did not change the growth of polymer per cycle, like in H_2SO_4. [11]

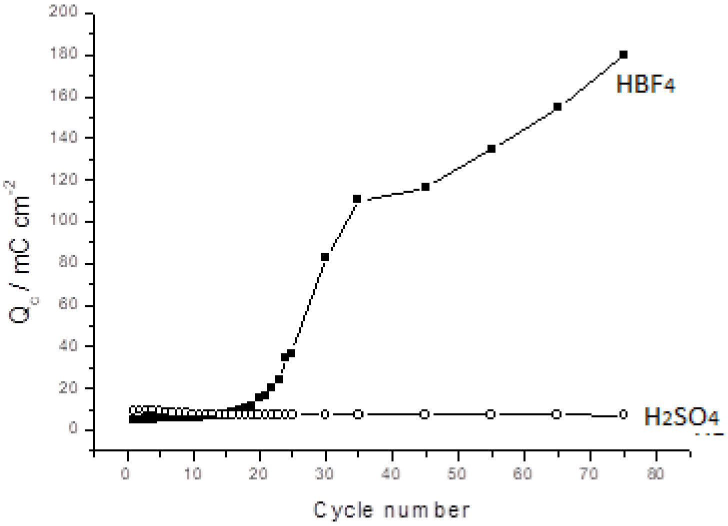

Figure 2. Variation of the cathodic charge density as a function of cycle number during electropolymerization of NMA on a Pt electrode surface in 1.0 M HBF_4 and 1.0 M H_2SO_4 solutions containing 0.1 M NMA.

3.2. Electrochemical characterization of PNMA on Pt surfaces

One anodic peak at about 0.41 V and the two cathodic ones at 0.30 V and 0.52 V are present in Figure 3(A). Both cyclic voltammograms showed a broad anodic wave centered at about 0.41 V ascribed to the oxidation of the polymer as well as electrolyte counter anions ingress or cations expulsion. The cathodic waves are responsible from the reduction of the polymer with a concomitant expulsion of anions or incorporation of cations. These reversible redox couples can be attributed to the reversible transition from LE to EM and from EM to PA in the polymer film.

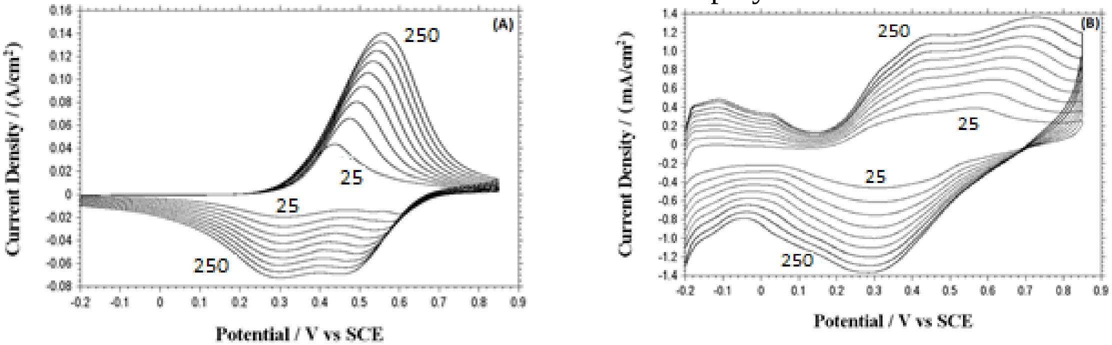

Figure 3. Cyclic voltammogram of PNMA coated Pt electrodes in monomer-free (A) 1.0 M HBF_4 and (B) 1.0 M H_2SO_4 solution in the potential region between -0.20 and 0.85 V vs. SCE at different scan rates (v = 25 to 250 mV s^{-1})

The PNMA films deposited on Pt surfaces were characterized by CV in a solution of 1.0 M HBF_4 solution. As seen in Figure 3, the electrochemical properties of the PNMA films are somewhat different for the second scan at different scan rates. While the cathodic peaks observed as two curves corresponding to the reduction process of the conducting EM to the insulating LE in 1.0 M HBF_4 solution shifted about 0.05 V at high scan rates, the Pt/PNMA electrode presented a sharper cathodic peak which somewhat shifted in 1.0 M H_2SO_4 solution at high scan rates.

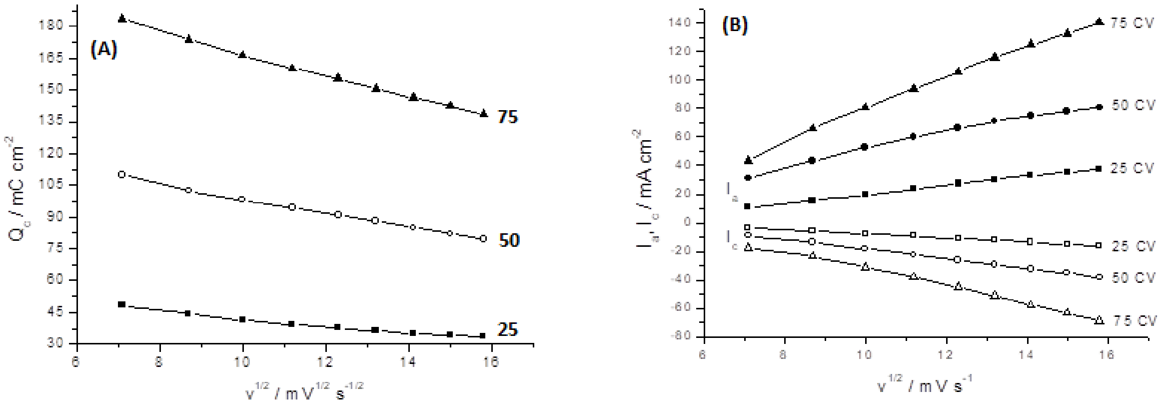

Figure 4. The dependence of (A) cathodic charge densities and (B) anodic and cathodic current values as a function of the square root of the scan rate from 50 to 250mV s^{-1} in the monomer-free electrolyte solution of 1.0 M HBF_4. (Films were obtained after 25, 50 and 75 cycles).

As can be seen in Figure 4, there is a linear dependency of cathodic current densities as a function of the square root of the scan rate from 50 to 250mV s^{-1}, which confirmed that the redox processes are diffusion-limited [4,10,11]. It can be concluded that the diffusion of counterions to the surface of the PNMA is the dominant parameter for determining the redox behaviour. For example, the different rates of diffusion for oxidation and reduction can reflect themselves as the variation of peak currents as shown in Figure 4 (B).

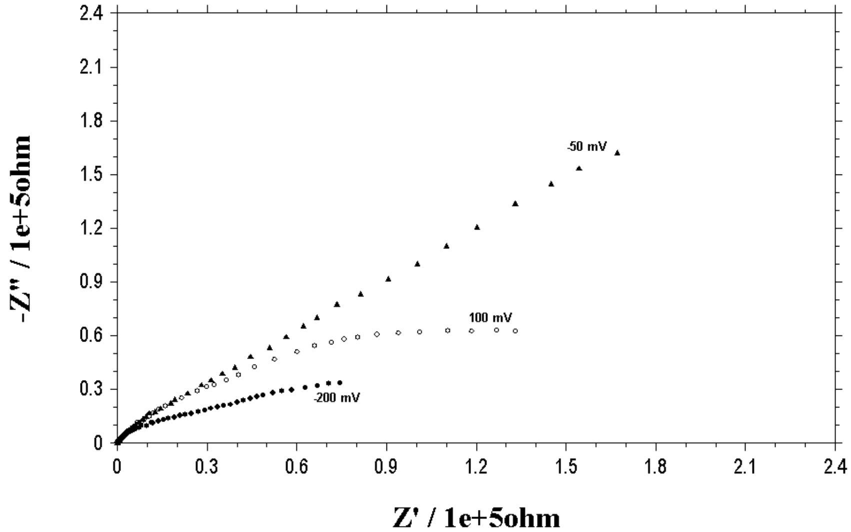

Figure 5. Impedance spectra of Pt/PNMA obtained in the monomer-free electrolyte solution of 1.0 M HBF_4 after applied external potentials of -200 mV, -50 mV and 100 mV vs SCE.

It is well known that the applied potentials can be influenced the electronic conductivity and the environments at the polymer - electrolyte interface [9] since the oxidation structures of PNMA can be changed by using various applied external dc potentials. Therefore, the effect of applied different external potentials can be monitored in the impedance spectra of PNMA coated Pt electrodes (see Figure 5). For EIS measurements, PNMA coated electrodes obtained after 75 growth cycles of CV were used. Nyquist diagrams (in the complex plan) recorded for the PNMA films in 1.0 M HBF_4 electrolyte solution at different electrode potentials (-200, -0.05, 100, 250, 400, 550, 700 and 850 mV vs SCE) were shown in Figure 5 and Figure 6.

As shown in the figures, only a semicircle impedance behaviour was obtained in the high-frequency region for all the curves recorded at applied negative potentials of -0.20 and -0.05 V as well as a positive potential of 100 mV. This phenomenon may be ascribed to the insulation property of a conducting polymer at these potentials [4, 10-13] which resulted in the reduction of the polymer with a concomitant expulsion of anions or incorporation of cations. The presence of the semicircles in the high frequency region can be attributed to the blocking property of a rough electrode [11,12]. This property makes the faradaic process of the ionic exchange slow at the polymer/electrolyte interface. The charge transfer resistance (R_{ct}) of the PNMA/electrolyte interface can be calculated from the diameter of the semicirle in the high-frequency region. The size of diameter, which is dependent on the applied dc potentials, increaed when the potential was increased from -200 mV to 100 mV. Based on the foregoing results, the semicircle observed in the high-frequency can be ascribed to the double-layer charging and discharging process [13]. However, the double-layer structure of PNMA was significantly affected by the applied dc potentials in the potential range from -200 mV to 100 mV. Upon moving from -200 mV to -50 mV, the R_{ct} is significantly increased due to uncomplete reduction of polymer, (i.e.. to the fully reduced state (LE). This increase of R_{ct} value is related to the lowering of the charger transfer rate which observed between the electrode and the solution. This low charge transfer can be resulted in due to the decrease of the polymer conductivity. As a conclusion, this phenomenon indicates that the electronic resistance of PNMA film has an important role in charge transport. Also, the ionic resistance is still much higher than electronic resistance.

There is an obvious difference between the R_{ct} values of the semicircles obtained in the impedance spectra of the PNMA electrodes obtained after applied potentials of -0.05 V and 0.10 V. As shown in Figure 5, the R_{ct} value obtained for -0.05 V is greater than the R_{ct} value recorded after applied 0.10 V. On the other hand, during increasing the potential up to 0.10 V, a decrease in R_{ct} value was observed due to the beginning of the polymer oxidation, which can be attributed to the transformation of PNMA from reduced LE form to the partially oxidized EM form.

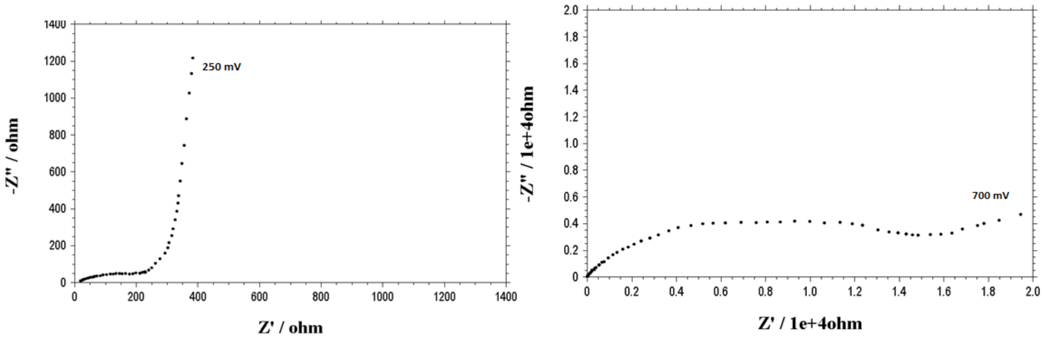

Figure 6. Impedance spectra of Pt/PNMA obtained in 1.0 M HBF_4 after applied potentials of 250, 700 mV vs SCE.

As increasing applied potential to 0.25 V, some appreciable changes were observed in Nyquist plots as shown in Figure 6. It can be concluded that the oxidation structures of PNMA film were firmly dependent on the applied external potentials. This factor, as expected, significantly influenced the electronic conductivity and the environments at the polymer/electrolyte interface. The changes in Nyquist plots can be attributable to the higher electronic conductivity, the charged polymer|electrolyte interface as well as the reversible redox characteristics of PNMA at more positive potentials. As depicted in Figure 6, the impedance curve of the PNMA film represented a single semicircle formed in the high frequency region and a straight line formed in the low frequency region, which are the characteristics behaviours of impedance spectra of a conducting polymer coated on metal electrodes in the asymmetric configuration. Similar behavior exhibits by all conducting polymer [1,3, 13]. But, when PNMA synthesized and electrochemically characterized in HBF4, they shown high growth and stable electroactivity.

The thickness of PNMA can be controlled by cyclic voltammetry (cycle number) during electropolymerization [1]. In this work, PNMA coated electrodes were obtained after 25, 50 and 75 growth cycles of CV were used for EIS measurements as depicted in Figure 7. The semicircle becomes smaller in the high-frequency region as a function of growth cycles upon moving from 25 to 75 cycles, which confirmed that the impedance responses of both double-layer and faradaic processes are dependent on the PNMA thickness. This results incicated that the impedance responces was affected by thickness of obtained PNMA on the Pt electrode surface. As the thickness of polymer incerase, the semicircles in the high frequency region was decreased which can be attributed to very low charge transfer resistance. Also, as polymer thickness increases, the angle observed in the low frequency region on the real axis increases towards ~90º after 75 cycles, indicating a smaller electron transfer resistance and easier redox transition for conductive PNMA coatings [1].

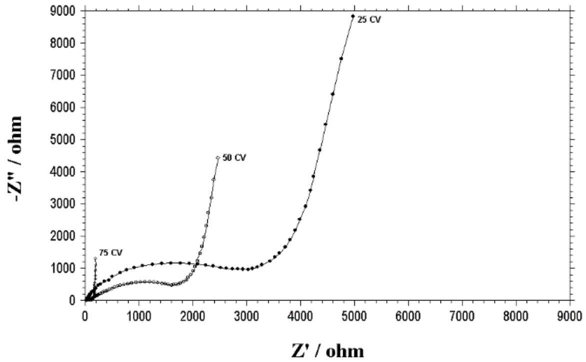

Figure 7. Impedance spectra of Pt/PNMA films obtained separately after 25, 50 and 75 growth cycles at a scan rate of 25 mV/s obtained in 1.0 M HBF_4 solution.

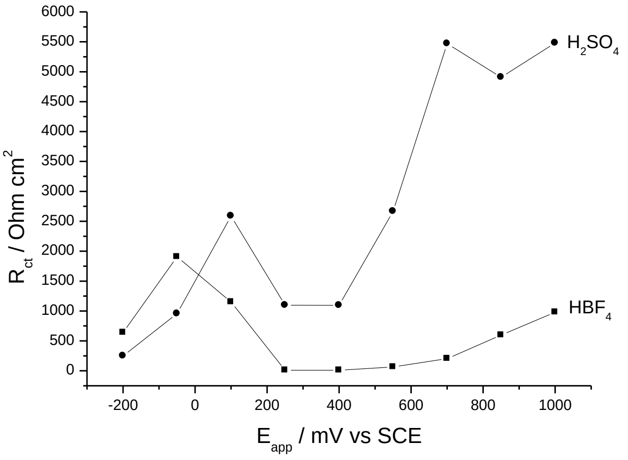

Figure 8. R_{ct} values determined from impedance spectra of Pt/PNMA films after applied external potentials in 1.0 M HBF_4 and 1.0 M H_2SO_4 solutions.

As can be seen in Figure 8, R_{ct} values of PNMA films are dramatically changes with an increase in the applied potentials in the monomer free various electrolyte solutions. The effect of electrolytes on R_{ct} values measured in the HBF_4 and H_2SO_4 electrolytes are negligible at potentials more negative than 100 mV vs SCE. On the other hand, R_{ct} vaues are significantly changed when the potentials are increased from 100 mV to 1000 mV. Therefore, the influences of the type and size of the anions on electroactivity and impedance behavior of PNMA are worthy of being studied.

4. CONCLUSİON

In conclusion, while the processes occurring at the polymer-electrolyte interfaces in Pt/PNMA substrates can be easily monitored in the high-frequency region of the impedance spectra, the faradaic redox transitions of PNMA were obtained in the low-frequency region for its different oxidation structures. PNMA obtained in HBF_4 electrolyte showed better electrochemical properties than those obtained in H_2SO_4 electrolyte.

References

1. C.- C. Hu, C.-H. Chu, *J. Electroanal. Chemistry*, 503 (2001) 105.
2. 2.T. Lindfors, A. Ivaska, *J. Electroanal. Chemistry*, 535 (2002) 65.
3. J. Arjomandi, H. Makhdomi, M. H. Parvin, *Synth. Metals*, 220 (2016) 123
4. M. Blomquist, T. Lindfors, L. Vahasalo, A. Pivrikas, A. Ivaska, *Synth. Metals*, 156 (2006) 549.
5. K. Brazdziuviene, I. Jureviciut, A. Malinauskas, *Electrochim. Acta*, 53 (2007) 785.
6. A. Hakimian, M. R. Nateghi, *Synth. Metals* 202 (2015) 1–7
7. G.A. Planes, J.L. Rodriguez, M.C. Miras, E. Pastor, C.A. Barbero, *Electrochim. Acta*, 122 (2014) 39.
8. K. Rouberg, L. Dunsch, *Electrochim. Acta* 44 (1999) 2061.
9. J. Yano, M. Kokura, K. Ogura, *J. Appl. Electrochemistry*, 24 (1994) 1164.
10. R. Pauliukaite, C. M. A. Brett, A. P. Monkman, *Electrochim. Acta*, 50 (2004) 167.
11. S. Ye, S. Besner, L.H. Dao, A.K. Vijh, *J. Electroanal. Chemistry*, 381 (1995) 71.
12. L. F. Marchesi, S. C. Jacumasso, R. C. Quintanilha, H. Winnischofer, M. Vidotti, *Electrochim. Acta,* 174 (2015) 864.
13. L. Niu, Q. Li, F. Wei, X. Chen, H. Wang, *J. Electroanal. Chemistry*, 544 (2003) 121.